Palmitate and Fructose Interact to Induce Human Hepatocytes to Produce Pro-Fibrotic Transcriptional Responses in Hepatic Stellate Cells Exposed to Conditioned Media

Ignazio S. Piras[a], **Glenn S. Gerhard[b]**, **Johanna K. DiStefano[a]**

[a]Translational Genomics Research Institute, Phoenix, AZ, USA

[b]Lewis Katz School of Medicine at Temple University, Philadelphia, PA, USA

Abstract

Background/Aims: Excessive consumption of dietary fat and sugar is associated with an elevated risk of nonalcoholic fatty liver disease (NAFLD). Hepatocytes exposed to saturated fat or sugar exert effects on nearby hepatic stellate cells (HSCs); however, the mechanisms by which this occurs are poorly understood. We sought to determine whether paracrine effects of hepatocytes exposed to palmitate and fructose produced profibrotic transcriptional responses in HSCs.

Methods: We performed expression profiling of mRNA and lncRNA from HSCs treated with conditioned media (CM) from human hepatocytes treated with palmitate (P), fructose (F), or both (PF).

Results: In HSCs exposed to CM from palmitate-treated hepatocytes, we identified 374 mRNAs and 607 lncRNAs showing significant differential expression ($\log_2$ foldchange |1|; FDR 0.05) compared to control cells. In HSCs exposed to CM from PF-treated hepatocytes, the number of differentially expressed genes was much higher (1198 mRNAs and 3348 lncRNAs); however, CM from fructose-treated hepatocytes elicited no significant changes in gene expression. Pathway analysis of differentially expressed genes showed enrichment for hepatic fibrosis and hepatic stellate cell activation in P- (FDR =1.30E-04) and PF-(FDR =9.24E-06) groups. We observed 71 lncRNA/nearby mRNA pairs showing differential expression under PF conditions. There were 90 mRNAs and 264 lncRNAs strongly correlated between the PF group and differentially expressed transcripts from a comparison of activated and quiescent HSCs, suggesting that some of the transcriptomic changes occurring in response to PF overlap with HSC activation.

Conclusion: The results reported here have implications for dietary modifications in the prevention and treatment of NAFLD.

Keywords

Hepatocyte; Fructose; Saturated fat; Transcriptomics; Hepatic steatosis; Hepatic stellate cell; Long noncoding RNA; Nonalcoholic fatty liver disease

Introduction

Nonalcoholic fatty liver disease (NAFLD) arises from excessive triacylglycerol deposition in hepatocytes and encompasses a histological spectrum with simple steatosis at one end and nonalcoholic steatohepatitis (NASH), often accompanied by fibrosis, at the other [1, 2]. Hepatic fat accumulation results from increased rates of *de novo* lipogenesis and hepatic fatty acid uptake or reduced levels of fatty acid oxidation and distribution of lipids from the liver to the circulation [3]. In the United States, NASH is the major cause of chronic liver disease and is poised to become the most common indication for liver transplantation [4].

Type 2 diabetes (T2D) and obesity increase the risk of developing NAFLD [5]. The close association among T2D, obesity, and NAFLD has likely antecedents in higher levels of overall daily energy intake and increased consumption of processed foods, which are major sources of sugar and saturated fat in the modern diet [6]. Indeed, high intake of saturated fat and cholesterol has been associated with hepatic steatosis [7-12]. In addition, dietary fructose has been associated with depletion of adenosine triphosphate, hepatic *de novo* lipogenesis, post-prandial hypertriglyceridemia [13, 14], and the development of NAFLD in the absence of traditional risk factors [15, 16]. Dietary fructose consumption has also been linked with severe fibrosis in NASH patients [17]. A number of different diet-induced animal models have been generated to investigate the effects of specific macronutrients on liver metabolism and NAFLD pathogenesis [18]. Many studies suggest a synergistic effect of high fat and fructose feeding on biological and histological parameters of NAFLD [19].

A number of studies have investigated changes in intercellular metabolism resulting from exposure to these nutrients in primary or immortalized hepatocytes and hepatic stellate cells (HSCs) [20-28]. HSCs are quiescent under physiological conditions, but are activated to a myofibroblastic state in response to injurious stimuli, whereupon they begin to secrete cytokines and components of the extracellular matrix (ECM). Under chronic conditions of hepatic inflammation, ECM components accumulate and eventually lead to hepatic scarring [29]. Conditioned media from primary human hepatocytes treated with palmitate was able to activate HSCs, decrease HSC apoptosis, and elicit changes in expression of pro-inflammatory and pro-fibrogenic genes [27]. Similarly, conditioned media from HepG2 cells treated with palmitate significantly increased alpha-SMA expression in immortalized human HSCs (LX-2 cells) [20]. Treatment of LX-2 cells with exosomes from palmitate-treated Huh7 cells resulted in significant changes in expression of genes related to fibrosis [23]. HepG2 cells treated with a combination of fructose, glucose, and fatty acids (palmitate and oleate) showed increased levels of triacylglycerols, total cholesterol, and inflammatory cytokines, as well as upregulated expression of genes involved in carbohydrate and lipid

metabolism [22], although fructose alone did not affect expression of lipogenic genes [28]. In mice, however, fructose-feeding induced expression of lipogenic genes, while inhibiting expression of genes involved in fatty acid oxidation [19]. In humans, fructose consumption for ten weeks led to increased hepatic *de novo* lipogenesis and 23-hour postprandial hypertriglyceridemia [14], suggesting that fructose may contribute to the development of NAFLD via the circulating lipid pool [8]. These data are consistent with recent evidence indicating that transcriptomic changes accompanying the early development of NAFLD occur predominantly in hepatocytes [24]. To date, however, the impact of palmitate- and fructose-treated human hepatocytes on transcriptomic changes in HSCs has not yet been characterized.

We hypothesized that fructose may amplify the effects of saturated fat by contributing to the biosynthesis of intracellular palmitate, leading to the enhanced expression of pro-fibrotic genes. In this study, we compared gene expression patterns in HSCs treated with conditioned media from primary human hepatocytes exposed to palmitate, fructose, or a combination of the two. We also compared a subset of RNAs showing differential expression in HSCs [30] treated with conditioned media from palmitate + fructose-treated hepatocytes with transcripts that were dysregulated in HSCs undergoing myofibroblastic transactivation, suggesting that these dietary macronutrients may contribute to fibrosis through HSC activation.

Materials and Methods

Cell treatments

Primary human hepatocytes (Thermo Fisher Scientific; Waltham, MA) were cultured in 500 µL William's E Medium supplemented with primary Hepatocyte Maintenance Supplement on collagen-coated 6-well plates. Culture medium was replaced the first day after thawing. LX-2 cells (Merck Millipore; Billerica, MA), an immortalized hepatic stellate cell line [31], were cultured in T-75 flasks containing 12 ml Dulbecco's Modified Eagle Medium (DMEM) supplemented with 2% fetal bovine serum (FBS). Culture medium was replaced the first day after seeding, and then every 72 hours. Cell line authentication was performed using short tandem repeat (STR) profiling (Cell Line Genetics; Madison, Wi), which confirmed the presence of a single cell line and alleles matching the known DNA fingerprint [32].

PHH were treated with 1 mM palmitate (P), 10 mM fructose (F), or a combination of 1 mM palmitate + 10 mM fructose (PF) for 48 hours. This concentration of palmitate was selected to approximate supraphysiological levels and promote triacylglycerol storage and lipotoxity [33, 34]. We assayed a range of concentrations for fructose treatment (5-25 mM), and found that 10 mM fructose optimally induced expression of lipogenic genes, similar to other findings [28]. A schematic overview of the experimental design is shown in Fig. 1A. Palmitate (Sigma-Aldrich; St. Louis, MO) was conjugated to bovine serum albumin (BSA; Omega Scientific; Tarzana, CA) at a final concentration of 1 mM palmitate and 1% BSA by heating at 37°C for 30 minutes prior to cell treatments [35]. Fructose (Sigma-Aldrich) was dissolved at a concentration of 300 mM in sterile water. Cells were serum-starved overnight, and then treated with either 1% BSA or 1 mM palmitate, in the presence or absence of 10 mM fructose for 24 and 48 hours. Oil Red O staining was performed to confirm uptake of

palmitate (Supplementary Fig. S1 – for all supplementary material see www.cellphysiolbiochem.com) [36].

LX-2 cells were seeded at 1 x 10^4 cell/well on 24-well plates coated with 85 μL of (1mg/mL) Matrigel Growth Factor Reduced (GFR) basement membrane matrix (Corning Inc; Corning, NY) and cultured for 72 hours at 37°C to induce a state resembling biological quiescence [37]. Media from treated PHH was collected and centrifuged twice at 1700 x g for 15 minutes to remove cell debris and aggregates. Cells were then treated with a cocktail containing 250 μL conditioned media from the different hepatocyte treatment groups and 250 μL LX-2 growth media and cultured for 48 hours.

Array hybridization and data analysis

Total RNA was extracted from three biological replicates for each treatment group using the RNeasy Mini Kit (Qiagen). All RNA preparations were diluted to 5 μg/μl. Samples were amplified and transcribed into fluorescent cRNA using a random priming method (Arraystar Flash RNA Labeling Kit [Arraystar; Rockville, MD]). Labeled cRNAs were purified using the RNeasy mini Kit (Qiagen) and the concentration and specific activity of the labeled cRNAs were measured using the NanoDrop ND-1000. One microgram of each labeled cRNA was fragmented and heated according to the manufacturer's protocol, and then added to the microarray slides. Slides were incubated for 17 hours at 65°C in an Agilent Hybridization Oven. The microarray used in this study was the Human LncRNA Microarray V4.0 (Arraystar), which allows detection of 40,173 lncRNAs and 20,730 protein-coding mRNAs. After washing and fixing, arrays were scanned using the Agilent DNA Microarray Scanner. Array images were analyzed using Agilent Feature Extraction software (version 11.0.1.1). Low quality mRNAs and lncRNAs were removed from further analysis, including those with at least three out of 15 samples with flags in "Present" (P) or "Marginal" (M) according to *GeneSpring GX v12.1*. Raw signal intensities for informative features were background-corrected and quantile-normalized using the R-package *limma* [38]. Quality controls (QC) were conducted using the R-package *arrayQualityMetrics* [39], inspecting heatmaps of inter-array expression distances, boxplots of expression values, and MAplots, which includes the log-intensity ratios (M-values) versus log-intensity averages (A-values). Differential expression analysis between treatment groups was conducted using a linear model as implemented in *limma*. P-values were adjusted for multiple testing using the False Discovery Rate method (FDR) [40]. Transcripts were considered to be differentially expressed if the FDR was <0.05 and the $\log_2$ fold change was |1|.

Pathway analysis

To interpret the biological significance of the microarray data, we uploaded the list of differentially expressed genes containing gene identifiers, FDR values, and $\log_2$FC into the Ingenuity Pathway Analysis (IPA) software (Qiagen). The "core analysis" function was applied to identify canonical pathways, upstream regulators, and gene networks relevant to the differentially expressed transcripts. The significance of the overrepresentation of differentially expressed genes in a pathway was assessed using a right-tailed Fisher's exact test and adjusting the p-values with the Benjamini-Hochberg method.

Co-expression analysis of lncRNAs and associated mRNAs

We mapped mRNAs located within 10 kb of differentially expressed lncRNAs, retaining the mRNAs/lncRNAs pairs showing statistically significant evidence for differential expression. We measured the relationship in expression between lncRNAs and associated mRNAs using Pearson's correlation and post hoc adjustment using the Benjamini-Hochberg method. Furthermore, we summarized the different classes of lncRNA/mRNA relationship (Bidirectional, Exon sense overlapping, Intron sense-overlapping, Intronic antisense, and Natural antisense) by concordant or discordant log_2 fold change direction.

Comparison with differentially expressed genes in activated hepatic stellate cells

We previously characterized mRNA and lncRNA expression changes that occurred during myofibroblastic activation of hepatic stellate cells using the same array platform [30]. We selected the differentially expressed genes from that study using the same cutoff applied in the current study (log_2 FC |1| and FDR < 0.05). Then, we intersected by probe ID the obtained list of genes with the differentially expressed genes from the palmitate + fructose treatment. The relationship between the two experiments was conducted computing the Pearson's correlation coefficient between the log_2 fold changes.

Results

Changes in RNA expression in LX-2 cells in response to palmitate and fructose

We first analyzed the pooled data obtained from the microarray experiments. Following removal of RNAs that did not meet quality control measures, 88.9% of the RNAs on the array were detected in HSCs, corresponding to 19,837 mRNAs and 32,471 lncRNAs. The mean normalized intensity was greater in mRNAs (log_2 normalized intensity = 9.592) compared to lncRNAs (log_2 normalized intensity =6.617), consistent with previous findings [30]. Sixty-eight percent of the detected lncRNAs were intergenic; the remainder of the lncRNAs had a bidirectional (5%), exon sense-overlapping (2%), intron sense-overlapping (3%), intronic (12%), or natural antisense (10%) orientation (Supplementary Fig. S2).

To establish baseline levels of potential residual media effects from palmitate (P) and fructose (F) on RNA expression in LX-2 cells, we compared mRNA and lncRNA levels in HSCs exposed to conditioned media from untreated hepatocytes with those from cells treated with palmitate and fructose (PF)-containing media from the hepatocyte-free control group (Fig. 1A). We identified 360 (162 upregulated and 198 downregulated) and 1207 (290 upregulated and 917 downregulated) differentially expressed mRNAs and lncRNAs, respectively, with log_2 fold-change >|1| and FDR <0.05 (Supplementary Fig. S3). To account for potential residual effects of palmitate and fructose not taken up by hepatocytes, we filtered all subsequent comparisons between treatment groups by this gene set. Filtering was conducted by probe ID to account for the presence of different transcript variants for the same gene.

We first assessed the effects of conditioned media from P-treated hepatocytes on transcriptomic changes in HSCs (Fig. 1B). We observed 374 differentially expressed mRNAs (176 upregulated and 198 downregulated) showing a log_2fold change |1| and FDR

<0.05 in LX-2 cells treated with conditioned media from hepatocytes exposed to palmitate compared to the control treatment (CT) cells (Supplementary Table S1). Transcripts showing the strongest evidence for differential expression (based on adjusted p-value) are shown in Table 1. Of the most dysregulated genes in Table 1, only *FNBP1L* has been linked with NAFLD in humans [24], although *PGF* [41], *SLC15B* [42, 43], and *WWP2* [44] have been associated with biological attributes of NAFLD in mouse and *in vitro* models.

We also observed 607 dysregulated lncRNAs: 459 upregulated and 148 downregulated molecules (Fig. 1B and Supplementary Table S2), compared to control conditions. Table 2 lists the lncRNAs showing the strongest evidence for differential expression between the two groups. Of note, the hypoxia upregulated 1 gene (*HYOU1*), associated with lncRNA RP11-110I1.6, is a known anti-apoptotic protein that plays a prominent role in hepatocyte survival [45].

In HSCs treated with conditioned media from hepatocytes exposed to 10 mM fructose, no statistically significant evidence (FDR <0.05) for differential mRNA or lncRNA expression was observed, indicating that at this concentration, fructose alone does not produce major transcriptional changes in our model (Fig. 1C). Despite the lack of significant changes in gene expression in the fructose group, treating HSCs with conditioned media from hepatocytes exposed to PF led to significant changes in expression for 1198 mRNAs, including 557 upregulated and 641 downregulated genes (Fig. 1D and Supplementary Table S3). Those transcripts showing the strongest evidence for differential expression are shown in Table 2. Not surprisingly, we observed substantial overlap between the differentially expressed genes shown in Tables 1 and 3 (P and PF-treated cells, respectively). Seven mRNAs (*MY03D*, *CREBF*, *DPP9-AS1*, *ZMAT4*, *MAT2A*, *OR6M1*, and *FB040*) were unique to the gene list from the combined PF-treated cells. We also observed differential expression of 3348 lncRNAs (1450 upregulated and 1898 downregulated) showing a $\log_2$ fold change >|1| and FDR <0.05 (Supplementary Table S4). LncRNAs showing the strongest evidence for differential abundance are shown in Table 4. In contrast to the overlap in differentially expressed mRNAs between the P and PF groups, only two lncRNAs, XLOC_006774 and G028271, were shared between the gene lists in Tables 2 and 4.

Given the overlap between mRNAs showing the strongest evidence for differential expression in Tables 1 and 3, we next sought to directly compare the datasets from the P and PF treatments (Fig. 2). In this comparison, we observed an overlap of 326 differentially expressed mRNAs between datasets (Supplementary Table S5). Of the shared differentially expressed genes, 276 showed higher variation in the PF group compared to the P group. Comparison of the lncRNAs from the P and PF treatment groups showed an overlap of 573 differentially expressed transcripts between the two conditions, with 522 showing higher expression in the PF group relative to the P group. We then compared the PF group with the P and CT groups combined. Using this approach, we identified 92 upregulated and 221 downregulated mRNAs and 480 upregulated and 1204 downregulated lncRNAs (Fig. 3).

Enriched biological pathway analysis of differentially expressed genes

We used functional enrichment analysis to identify biological attributes associated with the differentially expressed genes in individual group comparisons. The most significant canonical pathways involved in the different treatment conditions are shown in Table 5. Of note, in the comparison between HSCs exposed to conditioned media from untreated hepatocytes with HSCs treated with PF-containing media without hepatocytes, we observed enrichment in several biological pathways relevant to NAFLD, including *Hepatic Fibrosis/ Hepatic Stellate Cell Activation*, *LXR/RXR activation*, *TREM1 Signaling*, *Inhibition of Matrix Metalloprotease*, and *Hepatic Fibrosis Signaling Pathway*, suggesting that palmitate and fructose exert direct, i.e., not mediated by hepatocytes, effects on key fibrogenic pathways in HSCs. The most significant canonical pathway in the palmitate versus control treatment group was *Fatty Acid Activation*, while the most significant pathway in the PF group was *Hepatic Fibrosis/Hepatic Stellate Cell Activation*. Although the *Hepatic Fibrosis/ Hepatic Stellate Cell Activation* pathway was enriched across all comparisons, the PF treatment had the highest ratio of genes (12.9%) and the strongest significance (FDR = 9.24E-06) compared to the other groups.

Functional enrichment analysis of the 326 differentially expressed genes shared between the P and PF treatment groups identified *Fatty Acid* Activation as the top canonical pathway (P=1.89E-05). Interestingly, pathway analysis for the 48 and 872 differentially expressed genes unique to the P and PF treatment groups, respectively, identified *Hepatic Fibrosis/ Hepatic Stellate Cell Activation* as the top pathway for both gene sets suggesting that palmitate exposure drives the expression of this subset of genes.

Co-expression analysis of differentially expressed lncRNAs and mRNAs

We performed co-expression analysis of differentially expressed pairs of lncRNAs and nearby mRNAs to investigate the presence of potential regulatory mechanisms (Table 6). For the P versus CT comparison, we identified ten significant lncRNA/mRNA pairs. For the comparison of PF versus CT, we detected 71 significant mRNA/lncRNAs pairs (Supplementary Table S6); the ten most significant pairs are listed in Table 6. For the comparison of PF versus P + CT, we detected nine significant mRNA/lncRNAs pairs. The distribution of the transcriptional relationships in the PF dataset included 12 bidirectional, 1 exon sense overlapping, 7 intron sense overlapping, 27 intronic antisense, and 24 natural antisense lncRNAs (Supplementary Fig. S4); 56% of differentially expressed lncRNA/ nearby mRNA pairs in this comparison showed expression changes in opposing directions.

Differentially expressed RNAs in the PF treatment group are correlated with dysregulated genes in activated hepatic stellate cells

We previously characterized mRNA and lncRNA expression changes that occurred during myofibroblastic activation of HSCs [30]. Because the most significant pathway in the PF group was *Hepatic Fibrosis/Hepatic Stellate Cell Activation*, we compared this dataset with the RNAs that we found to be dysregulated between quiescent and activated HSCs (Fig. 4). We identified 675 probes that were differentially expressed in both analyses ($\log_2$FC |1|; FDR <0.05), corresponding to 301 mRNAs and 374 lncRNAs. A total of 480 probes showed a concordant $\log_2$FC, and of these, 343 up-regulated transcripts were located in a cluster

with highly correlated features (R = 0.745; P<2.2E-16). Pathway analysis of these 343 genes identified a number of overlapping canonical pathways, many of which are relevant to hepatic stellate cell function and activation (Fig. 5).

Discussion

We attempted to model the potential interaction between hepatocytes and HSC in response to common macronutrients. Although hepatocytes are the most abundant cell type in the liver, comprising approximately 80% of the total mass, the liver is comprised of multiple cell types, including HSCs, Kupffer cells, and sinusoidal endothelial cells [46]. In the presence of chronic excessive fat accumulation, hepatocytes generate toxic lipid metabolites, which contribute to ballooning degeneration, cell injury, and cell death. Hepatocytes also participate in the initiation and progression of fibrosis through complex processes involving nearby cells, particularly HSCs [47], which are triggered by hepatocyte injury [48]. In response to hepatic injury, quiescent HSCs transdifferentiate to an activated myofibroblastic state and begin to secrete cytokines and other molecules [49]. We found that conditioned media from hepatocytes treated with palmitate and fructose elicit changes in transcriptional programs associated with hepatic fibrosis in hepatic stellate cells. We also observed a cluster of 343 differentially expressed genes in cells treated with palmitate + fructose that were strongly correlated with genes upregulated during hepatic stellate cell activation, suggesting that paracrine factors released by hepatocytes in response to saturated fat and sugar may stimulate hepatic stellate cell activation and subsequent fibrogenesis in the liver.

Our results are consistent with previous *in vitro* studies that have investigated changes in cellular metabolism resulting from exposure to palmitate, fructose, or a combination of the two in primary or immortalized hepatocytes and HSCs. Conditioned media from HepG2 cells treated with palmitate significantly increased alpha-SMA expression in LX-2 cells, although LX-2 cells directly treated with palmitate did not show the same response, suggesting that a secondary metabolite from palmitate-treated HepG2 cells was responsible for HSC activation [20]. Windemuller et al. [26] showed that increasing the fructose to glucose ratio in Huh7 cells corresponded with elevated triacylglycerol and cholesterol synthesis, but this effect was not observed with increasing concentrations of glucose. In contrast, HepG2 cells treated with fructose did not show altered expression of lipogenic genes [22], although a combination of fructose, glucose, and fatty acids (palmitate and oleate) not only increased levels of triacylglycerols, total cholesterol, and inflammatory cytokines, but also upregulated expression of genes involved in carbohydrate and lipid metabolism [28]. These data are consistent with recent evidence indicating that transcriptomic changes accompanying the early development of NAFLD occur predominantly in hepatocytes [24]. The results reported here add to these findings by characterizing the impact of palmitate- and fructose-treated human hepatocytes on transcriptomic changes in HSCs.

Interestingly, our results did not show statistically significant changes in either mRNA or lncRNA expression in HSCs treated with conditioned media from hepatocytes exposed to fructose alone. This could be due to the concentration of fructose used in this study, 10 mM, which may be too low to induce metabolic effects in hepatocytes that lead to the secretion of

paracrine factors. Alternatively, treatment with fructose alone may not be sufficient to cause metabolic changes in liver cells. Some studies have shown that dietary fat produces stronger hepatic effects than added sugars [7, 8]. However, because fructose is known to stimulate *de novo* lipogenesis, and one of the major initial products of *de novo* lipogenesis is palmitate [7, 50, 51], it would be expected that fructose would exert metabolic effects similar to palmitate. We postulate that fructose, in the presence of palmitate, may amplify effects on gene expression by augmenting endogenous palmitate production in hepatocytes.

The roles of dietary saturated fat and added sugars in the pathogenesis of NAFLD is well recognized. Hepatic fat fraction has been associated with high intake of energy, total fat, and saturated fat in NAFLD [7] and NASH patients [52]. Saturated fat was also positively correlated with hepatic lipid content (β=0.45; p=0.03) and intrahepatic lipid (β=1.16; p=0.03), following adjustments for total energy intake, age, and BMI [7]. Saturated fat overfeeding had significantly stronger impacts on liver fat, plasma ALT levels, and atherogenic lipid levels compared to unsaturated fat [9, 12], which actually yielded a slight decrease in liver fat, improved lipid profiles, and no change in ALT [12]. Sugar overfeeding likewise led to a 33% increase in IHTG, specifically through the stimulation of *de novo* lipogenesis [9]. Hepatic *de novo* lipogenesis, lipid metabolism, and the 23-hour postprandial triacylglycerol AUC increased with fructose, but not glucose, consumption [14]. Rats fed a high fructose diet (60%) for 16 weeks developed both hepatic steatosis and dyslipidemia [8]. Combined, these findings provide evidence that dietary saturated fat and fructose specifically lead to changes in metabolic profiles relevant to the pathogenesis of NAFLD.

A novel aspect of the present work was a focus on differential expression of lncRNAs. We observed a significant overrepresentation of differentially expressed lncRNAs in the PF vs CT and PF vs P + CT groups (Chi-square P < 0.0001), but not in the P vs CT group (p = 0.341), suggesting that expression of these transcripts is more sensitive to paracrine effects from hepatocytes. In addition, co-expression analysis identified a number of lncRNA/mRNA pairs that were both differentially expressed suggesting the presence of potential regulatory mechanisms between co-expressed lncRNAs and nearby mRNA transcripts. Compared with protein-coding genes, lncRNAs show stronger tissue-specific patterns of expression [53], and these transcripts may associate with other co-expressed RNAs to produce similar phenotypic effects [54]. Finally, in the comparison with data from a transcriptomic analysis of activated HSCs [30], we observed overlap of 306 lncRNAs showing a $\log_2$FC concordance, including 258 lncRNAs that were highly correlated between the two datasets. To date, the majority of lncRNAs are unannotated, so the significance of these findings remains to be determined. However, because lncRNAs are known to influence expression of genes located in proximity (*cis*-acting) or elsewhere (*trans*-acting) through interactions with DNA, RNA, and protein [55], it is possible that some of the changes in expression of protein-coding genes are a direct result of regulatory lncRNAs.

The main limitation of this study is that the factors released by hepatocytes in response to palmitate and fructose that result in RNA expression changes in HSCs remain uncharacterized. A number of studies have sought to identify mechanisms by which hepatocytes may communicate a pro-fibrotic message to HSCs. For example, HepG2 cells treated with palmitate were found to release sphingosine 1-phosphate, which increased

expression of fibrogenic markers in LX-2 cells [20]. Another study showed that extracellular vesicles (EVs) were released from palmitate-treated mouse hepatocytes and subsequently internalized by both primary mouse HSCs and human LX-2 cells, resulting in increased expression of markers of HSC activation, migration, and proliferation [25]. In a similar study, exosomes from palmitate-treated Huh7 cells were shown to significantly alter expression of genes related to fibrosis in LX-2 cells [23]. Results from these two studies implicate a novel pathway by which lipotoxicity in hepatocytes may trigger fibrogenesis in HSCs.

We also recognize that palmitate may have cytotoxic effects on the liver and can result in cell injury and death [56]. Palmitate is known to activate hepatic stellate cells through mechanisms involving inflammasomes and hedgehog signaling [57]. In our studies, we did not observe increased cell death among hepatocytes treated with palmitate. Further, treatment of LX-2 cells with conditioned media from the palmitate + fructose no-cells control group did not increase expression of markers of activation, nor did morphological changes associated with transactivation to a myofibroblastic phenotype occur.

Conclusion

The results obtained in the current study demonstrate that conditioned media from hepatocytes treated with palmitate elicit changes in transcriptional programs associated with hepatic fibrosis in hepatic stellate cells, and these changes are amplified in the presence of fructose. The results have implications for dietary modifications in the prevention and treatment of NAFLD. Future investigations, including functional characterization of dysregulated transcripts and lncRNA-mRNA co-expressed networks, identification of factors released by hepatocytes in response to palmitate and fructose, and exploration of dietary interventions in appropriate animal models of NAFLD, will be important to extend these findings.

Supplementary Material

Refer to Web version on PubMed Central for supplementary material.

Acknowledgements

References

1. Matteoni CA, Younossi ZM, Gramlich T, Boparai N, Liu YC, McCullough AJ: Nonalcoholic fatty liver disease: a spectrum of clinical and pathological severity. Gastroenterology 1999;116:1413–1419. [PubMed: 10348825]

2. Rafiq N, Bai C, Fang Y, Srishord M, McCullough A, Gramlich T, et al.: Long-term follow-up of patients with nonalcoholic fatty liver. Clin Gastroenterol Hepatol 2009;7:234–238. [PubMed: 19049831]

3. Ipsen DH, Lykkesfeldt J, Tveden-Nyborg P: Molecular mechanisms of hepatic lipid accumulation in non-alcoholic fatty liver disease. Cell Mol Life Sci 2018;75:3313–3327. [PubMed: 29936596]

4. Charlton MR, Burns JM, Pedersen RA, Watt KD, Heimbach JK, Dierkhising RA: Frequency and outcomes of liver transplantation for nonalcoholic steatohepatitis in the United States. Gastroenterology 2011;141:1249–1253. [PubMed: 21726509]

5. Younossi ZM: Non-alcoholic fatty liver disease - A global public health perspective. J Hepatol 2019;70:531–544. [PubMed: 30414863]

6. Forouhi NG, Krauss RM, Taubes G, Willett W: Dietary fat and cardiometabolic health: evidence, controversies, and consensus for guidance. BMJ 2018;361:k2139. [PubMed: 29898882]

7. Cheng Y, Zhang K, Chen Y, Li Y, Li Y, Fu K, et al.: Associations between dietary nutrient intakes and hepatic lipid contents in NAFLD patiens quantified by 1H-MRS and Dual-Echo MRI. Nutrients 2016;8:527–545.

8. Jensen VS, Hvid H, Damgaard J, Nygaard H, Ingvorsen C, Wulff EM, et al.: Dietary fat stimulates development of NAFLD more potently than dietary fructose in Sprague-Dawley rats. Diabetol Metab Syndr 2018;10:4. [PubMed: 29410708]

9. Luukkonen PK, Sadevirta S, Zhou Y, Kayser B, Ali A, Ahonen L, et al.: Saturated Fat Is More Metabolically Harmful for the Human Liver Than Unsaturated Fat or Simple Sugars. Diabetes Care 2018;41:1732–1739. [PubMed: 29844096]

10. Parry SA, Hodson L: Influence of dietary macronutrients on liver fat accumulation and metabolism. J Investig Med 2017;65:1102–1115.

11. Puri P, Baillie RA, Wiest MM, Mirshahi F, Choudhury J, Cheung O, et al.: A lipidomic analysis of nonalcoholic fatty liver disease. Hepatology 2007;46:1081–1090. [PubMed: 17654743]

12. Rosqvist F, Kullberg J, Stahlman M, Cedernaes J, Heurling K, Johansson HE, et al.: Overeating saturated fat promotes fatty liver and ceramides compared to polyunsaturated fat: a randomized trial. J Clin Endocrinol Metab 2019;104:6207–6219. [PubMed: 31369090]

13. Jensen T, Abdelmalek MF, Sullivan S, Nadeau KJ, Green M, Roncal C, et al.: Fructose and sugar: A major mediator of non-alcoholic fatty liver disease. J Hepatol 2018;68:1063–1075. [PubMed: 29408694]

14. Stanhope KL, Schwarz JM, Keim NL, Griffen SC, Bremer AA, Graham JL, et al.: Consuming fructose-sweetened, not glucose-sweetened, beverages increases visceral adiposity and lipids and decreases insulin sensitivity in overweight/obese humans. J Clin Invest 2009;119:1322–1334. [PubMed: 19381015]

15. Abid A, Taha 0, Nseir W, Farah R, Grosovski M, Assy N: Soft drink consumption is associated with fatty liver disease independent of metabolic syndrome. J Hepatol 2009;51:918–924. [PubMed: 19765850]

16. Assy N, Nasser G, Kamayse I, Nseir W, Beniashvili Z, Djibre A, et al.: Soft drink consumption linked with fatty liver in the absence of traditional risk factors. Can J Gastroenterol 2008;22:811–816. [PubMed: 18925303]

17. Abdelmalek MF, Suzuki A, Guy C, Unalp-Arida A, Colvin R, Johnson RJ, et al.: Increased fructose consumption is associated with fibrosis severity in patients with nonalcoholic fatty liver disease. Hepatology 2010;51:1961–1971. [PubMed: 20301112]

18. Stephenson K, Kennedy L, Hargrove L, Demieville J, Thomson J, Alpini G, et al.: Updates on Dietary Models of Nonalcoholic Fatty Liver Disease: Current Studies and Insights. Gene Expr 2018;18:5–17. [PubMed: 29096730]

19. DiStefano JK: Fructose-mediated effects on gene expression and epigenetic mechanisms associated with NAFLD pathogenesis. Cell Mol Life Sci 2019;77:2079–2090.

20. Al Fadel F, Fayyaz S, Japtok L, Kleuser B: Involvement of Sphingosine 1-Phosphate in Palmitate-Induced Non-Alcoholic Fatty Liver Disease. Cell Physiol Biochem 2016;40:1637–1645. [PubMed: 28006772]

21. Hetherington AM, Sawyez CG, Zilberman E, Stoianov AM, Robson DL, Borradaile NM: Differential Lipotoxic Effects of Palmitate and Oleate in Activated Human Hepatic Stellate Cells and Epithelial Hepatoma Cells. Cell Physiol Biochem 2016;39:1648–1662. [PubMed: 27626926]

22. Hirahatake KM, Meissen JK, Fiehn 0, Adams SH: Comparative effects of fructose and glucose on lipogenic gene expression and intermediary metabolism in HepG2 liver cells. PLoS One 2011;6:e26583. [PubMed: 22096489]

23. Lee YS, Kim SY, Ko E, Lee JH, Yi HS, Yoo YJ, et al.: Exosomes derived from palmitic acid-treated hepatocytes induce fibrotic activation of hepatic stellate cells. Sci Rep 2017;7:3710. [PubMed: 28623272]

24. Li L, Liu H, Hu X, Huang Y, Wang Y, He Y, et al.: Identification of key genes in nonalcoholic fatty liver disease progression based on bioinformatics analysis. Mol Med Rep 2018;17:7708–7720. [PubMed: 29620197]

25. Povero D, Panera N, Eguchi A, Johnson CD, Papouchado BG, de Araujo Horcel L, et al.: Lipid-induced hepatocyte-derived extracellular vesicles regulate hepatic stellate cell via microRNAs targeting PPAR-gamma. Cell Mol Gastroenterol Hepatol 2015;1:646–663 e644. [PubMed: 26783552]

26. Windemuller F, Xu J, Rabinowitz SS, Hussain MM, Schwarz SM: Lipogenesis in Huh7 cells is promoted by increasing the fructose: Glucose molar ratio. World J Hepatol 2016;8:838–843. [PubMed: 27458503]

27. Wobser H, Dorn C, Weiss TS, Amann T, Bollheimer C, Buttner R, et al.: Lipid accumulation in hepatocytes induces fibrogenic activation of hepatic stellate cells. Cell Res 2009;19:996–1005. [PubMed: 19546889]

28. Zhao L, Guo X, Wang 0, Zhang H, Wang Y, Zhou F, et al.: Fructose and glucose combined with free fatty acids induce metabolic disorders in HepG2 cell: A new model to study the impacts of high-fructose/sucrose and high-fat diets *in vitro*. Mol Nutr Food Res 2016;60:909–921. [PubMed: 26763130]

29. Friedman SL: Hepatic stellate cells: protean, multifunctional, and enigmatic cells of the liver. Physiol Rev 2008;88:125–172. [PubMed: 18195085]

30. Gerhard GS, Davis B, Wu X, Hanson A, Wilhelmsen D, Piras IS, et al.: Differentially expressed mRNAs and lncRNAs shared between activated human hepatic stellate cells and nash fibrosis. Biochem Biophys Rep 2020;22:100753. [PubMed: 32258441]

31. Xu L, Hui AY, Albanis E, Arthur MJ, O'Byrne SM, Blaner WS, et al.: Human hepatic stellate cell lines, LX-1 and LX-2: new tools for analysis of hepatic fibrosis. Gut 2005;54:142–151. [PubMed: 15591520]

32. Weiskirchen R, Weimer J, Meurer SK, Kron A, Seipel B, Vater I, et al.: Genetic characteristics of the human hepatic stellate cell line LX-2. PLoS One 2013;8:e75692. [PubMed: 24116068]

33. Chu X, Jin Q, Chen H, Wood GC, Petrick A, Strodel W, et al.: CCL20 is up-regulated in non-alcoholic fatty liver disease fibrosis and is produced by hepatic stellate cells in response to fatty acid loading. J Transl Med 2018;16:108. [PubMed: 29690903]

34. Lee JY, Cho HK, Kwon YH: Palmitate induces insulin resistance without significant intracellular triglyceride accumulation in HepG2 cells. Metabolism 2010;59:927–934. [PubMed: 20006364]

35. Zhao NQ, Li XY, Wang L, Feng ZL, Li XF, Wen YF, et al.: Palmitate induces fat accumulation by activating C/EBPbeta-mediated G0S2 expression in HepG2 cells. World J Gastroenterol 2017;23:7705–7715. [PubMed: 29209111]

36. Yao HR, Liu J, Plumeri D, Cao YB, He T, Lin L, et al.: Lipotoxicity in HepG2 cells triggered by free fatty acids. Am J Transl Res 2011;3:284–291. [PubMed: 21654881]

37. Gerhard GS, Hanson A, Wilhelmsen D, Piras IS, Still CD, Chu X, et al.: AEBP1 expression increases with severity of fibrosis in NASH and is regulated by glucose, palmitate, and miR-372-3p. PLoS One 2019;14:e0219764. [PubMed: 31299062]

38. Ritchie ME, Phipson B, Wu D, Hu Y, Law CW, Shi W, et al.: limma powers differential expression analyses for RNA-sequencing and microarray studies. Nucleic Acids Res 2015;43:e47. [PubMed: 25605792]

39. Kauffmann A, Gentleman R, Huber W: arrayQualityMetrics--a bioconductor package for quality assessment of microarray data. Bioinformatics 2009;25:415–416. [PubMed: 19106121]

40. Benjamini Y, Hochberg Y: Controlling the False Discovery Rate: a Practical and Powerful Approach to Multiple Testing. J R Statist Soc B 1995;57:289–300.

41. Li X, Jin Q, Yao Q, Zhou Y, Zou Y, Li Z, et al.: Placental Growth Factor Contributes to Liver Inflammation, Angiogenesis, Fibrosis in Mice by Promoting Hepatic Macrophage Recruitment and Activation. Front Immunol 2017;8:801. [PubMed: 28744285]

42. Aguayo-Orozco A, Bois FY, Brunak S, Taboureau 0: Analysis of Time-Series Gene Expression Data to Explore Mechanisms of Chemical-Induced Hepatic Steatosis Toxicity. Front Genet 2018;9:396. [PubMed: 30279702]

43. Ijssennagger N, Janssen AWF, Milona A, Ramos Pittol JM, Hollman DAA, Mokry M, et al.: Gene expression profiling in human precision cut liver slices in response to the FXR agonist obeticholic acid. J Hepatol 2016;64:1158–1166. [PubMed: 26812075]

44. Ge MX, Liu HT, Zhang N, Niu WX, Lu ZN, Bao YY, et al.: Costunolide represses hepatic fibrosis through WW domain-containing protein 2-mediated Notch3 degradation. Br J Pharmacol 2020;177:372–387. [PubMed: 31621893]

45. Haimerl F, Erhardt A, Sass G, Tiegs G: Down-regulation of the de-ubiquitinating enzyme ubiquitin-specific protease 2 contributes to tumor necrosis factor-alpha-induced hepatocyte survival. J Biol Chem 2009;284:495–504. [PubMed: 19001362]

46. Gao B, Jeong WI, Tian Z: Liver: An organ with predominant innate immunity. Hepatology 2008;47:729–736. [PubMed: 18167066]

47. Magee N, Zou A, Zhang Y: Pathogenesis of Nonalcoholic Steatohepatitis: Interactions between Liver Parenchymal and Nonparenchymal Cells. Biomed Res Int 2016;2016:5170402. [PubMed: 27822476]

48. Tu T, Calabro SR, Lee A, Maczurek AE, Budzinska MA, Warner FJ, et al.: Hepatocytes in liver injury: Victim, bystander, or accomplice in progressive fibrosis? J Gastroenterol Hepatol 2015;30:1696–1704. [PubMed: 26239824]

49. Tsuchida T, Friedman SL: Mechanisms of hepatic stellate cell activation. Nat Rev Gastroenterol Hepatol 2017;14:397–411. [PubMed: 28487545]

50. Jacobs S, Jager S, Jansen E, Peter A, Stefan N, Boeing H, et al.: Associations of Erythrocyte Fatty Acids in the De Novo Lipogenesis Pathway with Proxies of Liver Fat Accumulation in the EPIC-Potsdam Study. PLoS One 2015;10:e0127368. [PubMed: 25984792]

51. Yilmaz M, Claiborn KC, Hotamisligil GS: De Novo Lipogenesis Products and Endogenous Lipokines. Diabetes 2016;65:1800–1807. [PubMed: 27288005]

52. Musso G, Gambino R, De Michieli F, Cassader M, Rizzetto M, Durazzo M, et al.: Dietary habits and their relations to insulin resistance and postprandial lipemia in nonalcoholic steatohepatitis. Hepatology 2003;37:909–916. [PubMed: 12668986]

53. Kapusta A, Kronenberg Z, Lynch VJ, Zhuo X, Ramsay L, Bourque G, et al.: Transposable elements are major contributors to the origin, diversification, and regulation of vertebrate long noncoding RNAs. PLoS Genet 2013;9:e1003470. [PubMed: 23637635]

54. Cabili MN, Trapnell C, Goff L, Koziol M, Tazon-Vega B, Rege A, et al.: Integrative annotation of human large intergenic noncoding RNAs reveals global properties and specific subclasses. Genes Dev 2011;25:1915–1927. [PubMed: 21890647]

55. Chen LL: Linking Long Noncoding RNA Localization and Function. Trends Biochem Sci 2016;41:761–772. [PubMed: 27499234]

56. Arain SQ, Talpur FN, Channa NA, Ali MS, Afridi HI: Serum lipid profile as a marker of liver impairment in hepatitis B Cirrhosis patients. Lipids Health Dis 2017;16:51. [PubMed: 28249586]

57. Duan NN, Liu XJ, Wu J: Palmitic acid elicits hepatic stellate cell activation through inflammasomes and hedgehog signaling. Life Sci 2017;176:42–53. [PubMed: 28322865]
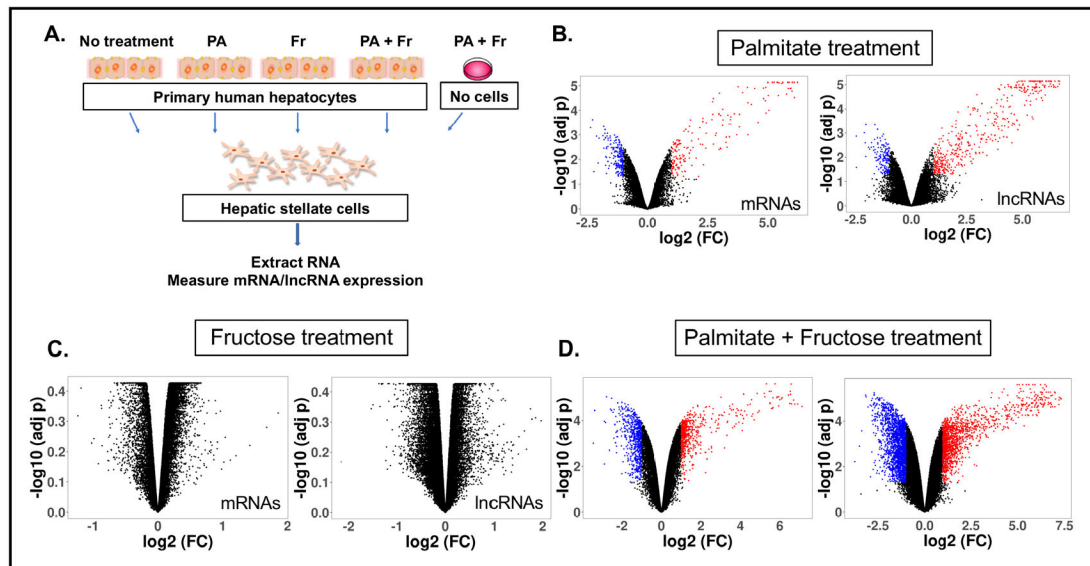
Fig. 1.
Differentially expressed transcripts in HSCs exposed to conditioned media from treated hepatocytes. A) Overview of cell treatment strategy. Hepatocytes (PHHs) were treated with 1 mM palmitate, 10 mM fructose, or a combination of 1 mM palmitate and 10 mM fructose for 48 hours. LX-2 cells induced to achieve a quiescent phenotype [37] were then treated with hepatocyte-derived conditioned media for an additional 48 hours. Following stimulation with conditioned media, RNA was extracted from cells as described in the Methods section and quantitated using array hybridization. Volcano plots for HSCs exposed to conditioned media from hepatocytes treated with B) 1 mM palmitate, C) 10 mM fructose, or D) 1 mM palmitate + 10 mM fructose were performed to identify differentially expressed mRNAs and lncRNAs compared to the control treatment group. In the x-axis the is reported the $\log_2$ fold change, and in the y-axis the $-\log_{10}(\text{adj p})$. Data points in red represent significantly upregulated transcripts, while those in blue represent significantly downregulated transcripts ($\log_2$ fold change ꙳|1|; adj p<0.05). Black-colored data points represent RNAs not showing statistically significant evidence for differential expression between treatment groups.
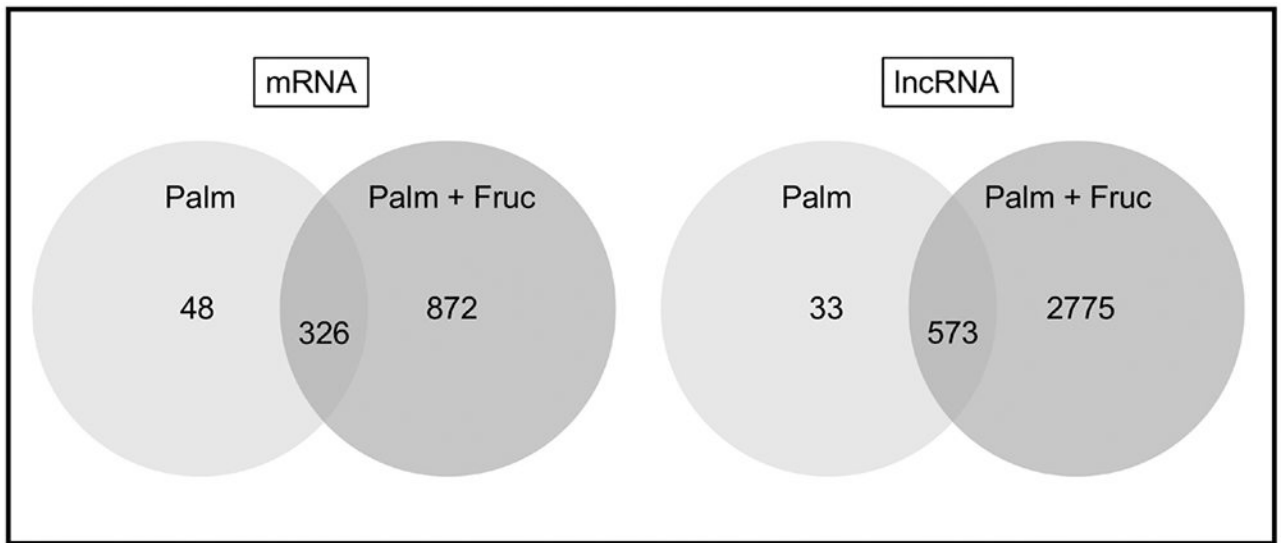
Fig. 2.
Overlap between data sets from palmitate-only and palmitate + fructose treatment groups.
Venn diagrams were generated to show the overlap between the two treatment conditions for
mRNAs and lncRNAs.
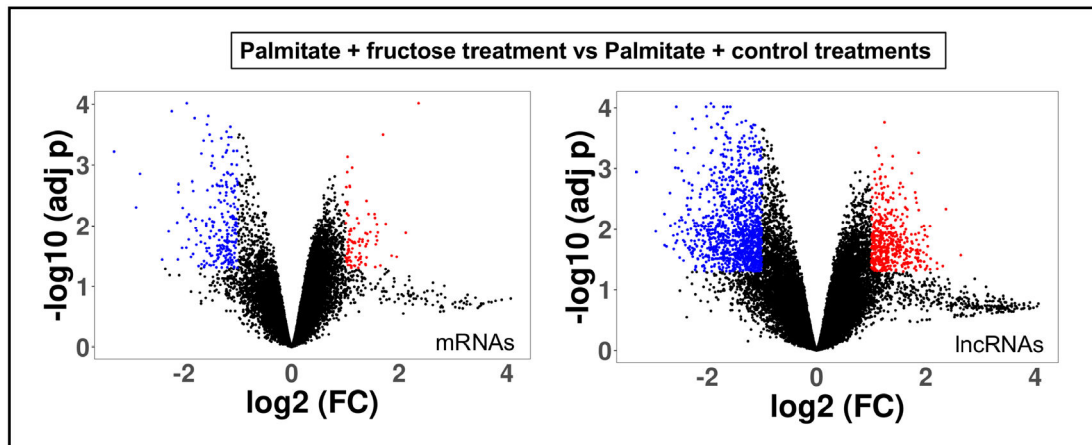
Fig. 3.

Differentially expressed transcripts in HSCs exposed to conditioned media from PF-treated hepatocytes compared to P + CT hepatocytes. Volcano plot for HSCs exposed to conditioned media from hepatocytes treated with 1 mM palmitate and 10 mM fructose versus the combined gene sets from palmitate-only and control-treated cells was performed to identify differentially expressed mRNAs and lncRNAs between groups. In the x-axis the is reported the $\log_2$ fold change, in the y-axis the $-\log_{10}$(adj p) . Data points in red represent significantly upregulated transcripts, while those in green represent significantly downregulated transcripts ($\log_2$ fold change |1|; adj p<0.05). Black-colored data points represent RNAs not showing statistically significant evidence for differential expression between treatment groups.
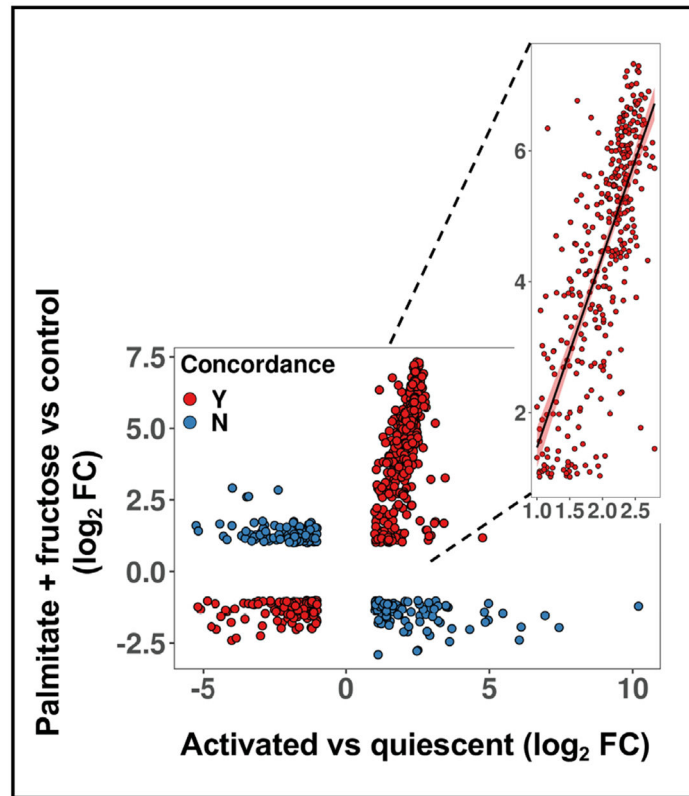
Fig. 4.

Comparison of differentially expressed RNAs in the PF treatment group with dysregulated genes in activated hepatic stellate cells. A) 675 probes were differentially expressed in both analyses ($\log_2$FC |1|; FDR <0.05). A total of 480 probes showed a concordant $\log_2$FC (indicated by red dots). The upregulated transcripts located in a cluster with highly correlated features are expanded.

Fig. 5.
Pathway analysis of highly correlated transcripts); overlapping significant canonical
pathways identified by IPA are shown.

Table 1.

mRNAs showing strongest evidence for differential expression in LX-2 cells exposed to conditioned media from palmitate-treated hepatocytes.

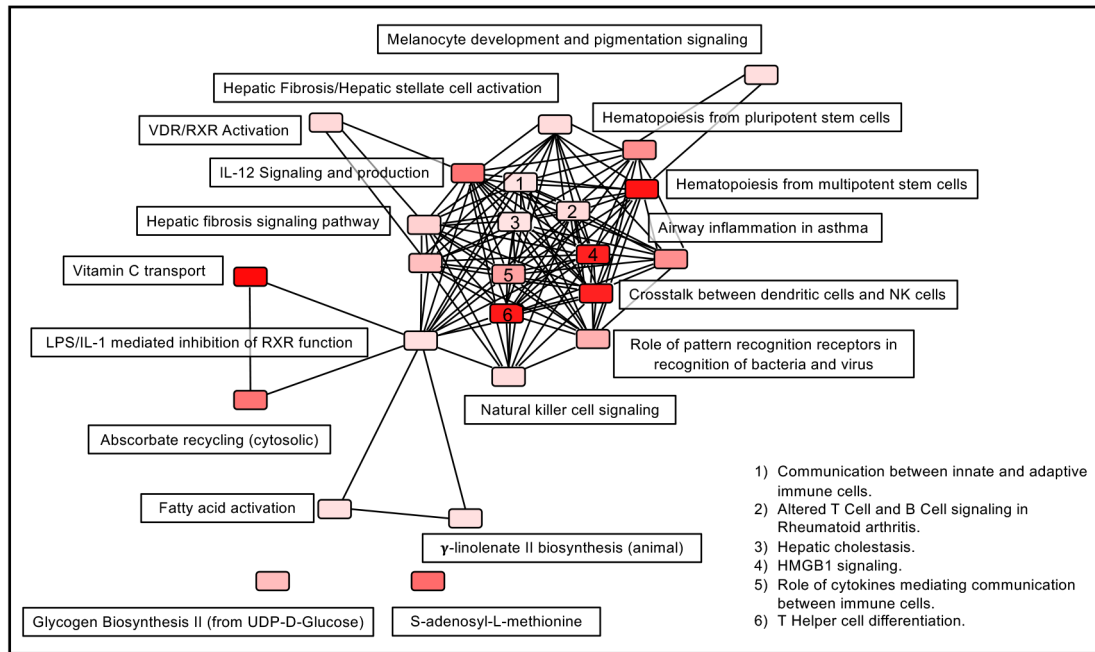| ID	Gene Symbol	Description	Normalized intensity			
			FDR	Log$_2$FC	1 mM[*]	0 mM[*]
NM_003696	OR6A2	olfactory receptor family 6 subfamily A member 2	7.3E-06	6.23	15.37	9.12
NM_001012970	C1orf100	chromosome 1 open reading frame 100	7.3E-06	6.10	12.50	6.12
NM_001135995	ATXN3L	ataxin 3-like	7.3E-06	6.01	14.87	8.84
NM_002632	PGF	placental growth factor	7.3E-06	5.89	13.91	7.97
NM_001098814	SRL	sarcalumenin	7.3E-06	5.83	12.53	6.55
NM_000899	KITLG	KIT ligand	7.3E-06	5.40	15.49	10.08
uc011dig.1	OFCC1	orofacial cleft 1 candidate 1	7.3E-06	5.38	16.24	10.86
NM_173848	RALYL	RALY RNA binding protein-like	7.3E-06	5.26	11.38	5.91
NM_001195581	ARL14EPL	ADP ribosylation factor like GTPase 14 effector protein like	7.3E-06	5.19	11.75	646
NM_153813	ZFPM1	zinc finger protein, FOG family member 1	7.3E-06	5.00	12.40	7.32
NM_178859	SLC51B	solute carrier family 51 beta subunit	7.3E-06	5.62	13.42	7.73
NM_018348	CMTR2	cap methyltransferase 2	7.5E-06	5.00	15.61	10.59
NM_002987	CCL17	chemokine (C-C motif) ligand 17	8.0E-06	5.58	11.71	5.93
NM_001164473	FNBP1L	formin binding protein 1-like	1.1E-05	3.77	12.10	8.30
NM_153695	ZNF367	zinc finger protein 367	1.2E-05	4.92	13.89	8.96
NM_007014	WWP2	WW domain containing E3 ubiquitin protein ligase 2	1.2E-05	4.15	12.54	8.37
NM_002103	GYS1	glycogen synthase 1	1.3E-05	4.82	14.77	9.95
NM_001005168	OR52E8	olfactory receptor family 52 subfamily E member 8	1.3E-05	5.96	11.63	5.34
ENST00000284481	C8orf12	Chromosome 8 open reading frame 12	1.3E-05	5.93	13.49	6.59
NM_001003819	TRIM6-TRIM34	TRIM6-TRIM34 readthrough	1.3E-05	5.85	12.49	6.52

[*] concentration of palmitate used to treat PHH

Table 2.

Top mRNAs dysregulated in LX-2 cells exposed to conditioned media from PF-treated hepatocytes

ID	Gene Symbol	Description		Normalized intensity		
			FDR	Log$_2$FC	treated	control
NM_018348	CMTR2	cap methyltransferase 2	2.5E-06	5.32	15.61	10.59
NM_000899	KITLG	KIT ligand	2.5E-06	5.76	15.49	10.08
NM_003696	OR6A2	olfactory receptor family 6 subfamily A member 2	2.6E-06	6.58	15.37	9.12
uc011dig.1	0FCC1	orofacial cleft 1 candidate 1	5.4E-06	5.47	16.24	10.86
NM_001135995	ATXN3L	ataxin 3-like	5.4E-06	6.53	14.87	8.84
NM_017433	MYO3A	myosin IIIA	5.4E-06	5.56	15.79	10.37
NM_153607	CREBRF	CREB3 regulatory factor	6.6E-06	4.85	15.49	11.03
NM_002103	GYS1	glycogen synthase 1	6.6E-06	5.21	14.77	9.95
NM_001242901	DPP9-AS1	DPP9 antisense RNA 1	7.0E-06	4.16	17.33	13.17
NM_001012970	C1orf100	chromosome 1 open reading frame 100	7.2E-06	6.54	12.50	6.12
NM_001098814	SRL	sarcalumenin	7.7E-06	6.44	12.52	6.55
NM_024645	ZMAT4	zinc finger, matrin-type 4	9.2E-06	−2.78	8.16	10.57
NM_153695	ZNF367	zinc finger protein 367	9.2E-06	5.24	13.89	8.96
NM_001195581	ARL14EPL	ADP ribosylation factor like GTPase 14 effector protein like	9.2E-06	5.87	11.75	6.46
NM_178859	SLC51B	solute carrier family 51 beta subunit	9.2E-06	5.94	13.42	7.73
NM_005911	MAT2A	methionine adenosyltransferase II, alpha	9.6E-06	3.02	15.71	13.01
NM_002987	CCL17	chemokine (C-C motif) ligand 17	1.0E-05	6.12	12.26	5.93
NM_173848	RALYL	RALY RNA binding protein-like	1.0E-05	5.85	11.97	5.91
NM_001005325	OR6M1	olfactory receptor family 6 subfamily M member 1	1.0E-05	5.65	10.27	3.75
NM_016298	FBXO40	F-box protein 40	1.1E-05	6.08	13.52	7.34

Table 3.

lncRNAs showing strongest evidence for differential expression in LX-2 cells exposed to conditioned media from palmitate-treated hepatocytes.

ID	Gene Symbol	Associated Gene	Normalized intensity			
			FDR	Log$_2$FC	1 mM[*]	0 mM[*]
T173832	G040382		7.3E-06	6.67	14.37	7.64
NR_105039	LOC101927488		7.3E-06	6.61	14.06	7.36
T314169	G073685		7.3E-06	6.46	14.85	8.36
ENST00000580967	RP11-527H14.2		7.3E-06	6.46	14.83	8.33
ENST00000597156	CTD-3193013.11	Proline rich 36 (PRR36)	7.3E-06	6.30	14.03	7.65
NR_125419	LOC101927543	Syntrophin beta 1 (SNTB1)	7.3E-06	6.24	14.92	8.65
TCONS_00018312	XLOC_008586		7.3E-06	6.22	15.38	9.15
TCONS_00014675	XLOC_006774		7.3E-06	6.16	16.09	9.93
ENST00000416861	AC009502.4		7.3E-06	6.07	15.56	9.49
TCONS_12_00017992	XLOC_12_009508		7.3E-06	6.05	14.70	8.63
T119684	G028271	Secretory carrier membrane protein 5 (SCAMP5)	7.3E-06	5.90	14.26	8.34
ENST00000566418	RP11-686F15.2		7.3E-06	5.87	14.11	8.17
T271295	G062886		7.3E-06	5.87	12.63	6.64
ENST00000423020	RP5-963E22.4		7.3E-06	5.87	14.40	8.49
TCONS_00014959	XLOC_007038		7.3E-06	5.80	13.81	7.91
T372494	G087836		7.3E-06	5.78	13.94	8.10
TCONS_00000947	XLOC_000202		7.3E-06	5.75	14.51	8.72
NR_002165	HMGB3P1		7.3E-06	5.75	13.14	7.28
T085588	G019854		7.3E-06	5.74	12.14	6.16
ENST00000531886	RP11-110I1.6	Hypoxia upregulated 1 (HYOU1)	7.3E-06	5.68	13.52	7.78

[*] concentration of palmitate used to treat PHH

Table 4.

Top lncRNAs dysregulated in LX-2 cells exposed to conditioned media from PF-treated hepatocytes

ID	Gene Symbol	Associated Gene	FDR	Log$_2$FC	treated	control
					Normalized intensity	
ENST00000445280	RP11-165J3.6		2.5E-06	4.98	17.25	12.26
ENST00000527239	CTD-2589M5.4		2.5E-06	5.09	16.62	11.54
TCONS_00019584	XLOC_009382		2.5E-06	5.26	17.01	11.74
NR_024330	SPACA6P		2.5E-06	5.47	16.22	10.75
T161198	G037238		2.5E-06	5.59	16.71	11.11
T169470	G039345	Adhesion G protein-coupled receptor (ADGRL1)	2.5E-06	5.61	17.01	11.40
uc.243+	uc.243	zinc finger homeobox 4 (ZFHX4)	2.5E-06	5.81	15.74	9.92
T343400	G080682		2.5E-06	5.92	15.89	9.96
uc001oou.3	BC064339	two pore segment channel 2 (TPCN2)	2.5E-06	6.22	16.21	10.00
TCONS_00014675	XLOC_006774		2.5E-06	6.46	16.40	9.93
ENST00000431001	RP11-439H9.1		2.9E-06	6.54	16.23	9.67
ENST00000579499	CTB-58E17.9	Myeloid/lymphoid or mixed-lineage leukemia; translocated to 6 (MLLT6)	3.5E-06	6.35	15.49	9.10
T198560	G045831	excision repair cross-complementing rodent repair deficiency, complementation group 3 (ERCC3)	3.7E-06	5.14	17.10	11.95
T256902	G059221		3.8E-06	4.27	16.74	12.49
ENST00000464125	RP11-475023.3	family with sequence similarity 107 member A (FAM107A)	3.8E-06	5.67	16.33	10.68
T119684	G028271	secretory carrier membrane protein 5 (SCAMP5)	4.1E-06	6.43	14.81	8.34
T280062	G065072		4.9E-06	5.18	16.67	11.47
T253780	G058468		4.9E-06	5.31	12.05	6.56
T264852	G061132		5.4E-06	−4.09	3.76	8.68
T379563	G089863		5.4E-06	4.18	17.02	12.86

Table 5.

Functional enrichment analysis of differentially expressed genes in individual group comparisons

Group	Ingenuity Canonical Pathway	FDR	Genes
NC vs CT	Hepatic Fibrosis / Hepatic Stellate Cell Activation	2.22E-06	COL11A1, COL13A1, COL17A1, COL1A2, COL21A1, CXCL2, CXCL8, IGFBP4, IL1A, IL1B, MMP1, MMP9, VEGFA[1]
	LXR/RXR Activation	2.97E-04	BCA1, IL1A, IL1B, MMP9, MYLIP, NR1H4, SAA1, SAA2
	TREM1 Signaling	6.23E-04	CXCL2, CXCL8, IL1B, IRAK1, NLRP3, TREM1
	Inhibition of Matrix Metalloprotease	2.06E-03	MMP1, MMP28, MMP9, TFPI2
	Hepatic Fibrosis Signaling Pathway	5.71E-03	CCND1, COL1A2, CXCL8, IL1A, IL1B, IRAK1, ITGA3, MAPK13, MMP1, OPN1SW, RHOB, VEGFA[1]
P vs CT	Fatty Acid Activation	3.28E-05	ACSL6, SLC27A2, SLC27A5, SLC27A
	γ-linolenate Biosynthesis II (Animals)	1.04E-04	ACSL6, SLC27A2, SLC27A5, SLC27A6
	Mitochondrial L-carnitine Shuttle Pathway	1.04E-04	ACSL6, SLC27A2, SLC27A5, SLC27A6
	Hepatic Fibrosis / Hepatic Stellate Cell Activation	1.30E-04	AGTR1, BAMBI, COL15A1, COL3A1, EDNRB, FGF1, FN1, IGFBP5, IL4, PGF, SERPINE1
	LPS/IL-1 Mediated Inhibition of RXR Function	6.38E-04	ACOX2, ACSL6, CYP2C8, FABP7, GSTM3, NDST4, PPARGC1A, SLC27A2, SLC27A5, SLC27A6, SREBF1
PF vs CT	Hepatic Fibrosis / Hepatic Stellate Cell Activation	9.24E-06	CD14, COL16A1, COL22A1, COL24A1, COL3A1, COL7A1, COL8A2, COL9A1, ECE1, EGFR, FGF1, FGFR1, FN1, ICAM1, IGF1, IGFBP3, IL4, MYH11, PGF, SERPINE1, TGFB3, TGFBR2, VEGFA[2] VEGFC
	LPS/IL-1 Mediated Inhibition of RXR Function	2.68E-05	ACOX2, ACSBG1, ACSL6, ALDH1A1, ALDH1L2, CD14, CHST11, CYP2C8, FABP7, GSTM3, GSTO2, HMGCS1, HS3ST6, ILI8, LIPC, MAOB, MGST1, NDST1, NDST4, NR1I3, PPARGC1A, SLC27A2, SLC27A5, SLC27A6, SREBF1, SULT1E1
	Neuroinflammation Signaling Pathway	4.71E-05	ATF4, BIRC8, CD200, CXCL12, GABRB2, GABRE, GABRG1, GABRG2, GABRQ, HLA-DMB, HMOX1, ICAM1, IFNA8, IL18, IL4, KCNJ6, MMP3, NOX4, PIK3C2B, PIK3R3, PLA2G10, PLA2G2A, PLA2G2E, PLA2G4A, PLA2G5, PYCARD, SLC1A3, TGFB3, TGFBR2, TLR10, TLR3
	Unfolded protein response	5.70E-05	ATF4, CEBPB, CEBPG, EIF2AK3, HSPA1A/HSPA1B, HSPA6, INSIG1, MAP3K5, PPP1R15A, SREBF1, XBP1
	Phospholipases	1.74E-04	HMOX1, LIPC, PLA2G10, PLA2G2A, PLA2G2C, PLA2G2E, PLA2G4A, PLA2G5, PLB1, PLCD1, PLCE1
PF vs P +CT	Breast Cancer Regulation by Stathmin1	2.18E-04	ADGRE3, ADGRF3, ADGRG7, ADGRV1, CCR10, CHRM1, DRD1, GPR141, GPR149, GPR61, HCRTR2, HTR2A, IGF1, NPFFR1, NPY2R, P2RY14, PROKR1, TUBB1
	Graft-versus-Host Disease Signaling	2.36E-03	FCER1G, KIR2DL1/KIR2DL3, PRF1, TRA
	Fc Epsilon RI Signaling)	2.54E-03	BTK, FCER1G, PLA2G10, PLA2G2A, PLA2G2E, VAV3
	eNOS Signaling	2.70E-03	CHRM1, CHRNA3, CHRNB4, CNGB3, GUCY1A1, HSPA6, NOSTRIN
	GP6 Signaling Pathway	2.76E-03	BTK, COL22A1, COL24A1, COL3A1, COL9A1, FCER1G

Table 6.

Co-expression analysis of lncRNAs and associated mRNAs in different comparison groups.

lncRNAs			Associated mRNAs			Relationship
ID	Log$_2$FC	p$_{adj}$	ID	Log$_2$FC	p$_{adj}$	
P vs CT						
HAND2-AS1	−2.04	4.57E-04	HAND2	−1.53	1.72E-03	bidirectional
uc.243	5.39	7.29E-06	ZFHX4	−1.07	4.18E-03	intron sense-overlapping
EGFL8	4.65	1.31E-05	NG3	1.74	5.59E-03	exon sense-overlapping
ZFHX4-AS1	−1.48	4.03E-03	ZFHX4	−1.07	4.18E-03	intronic antisense
RP11-234O6.2	−1.27	1.40E-02	FSTL5	−1.23	3.11E-02	natural antisense
uc.447	3.95	6.97E-04	ZNF536	−1.10	1.74E-02	intron sense-overlapping
THSD4-AS2	−1.50	1.37E-02	THSD4	3.13	8.91E-05	intronic antisense
AK091275	1.09	9.89E-03	SORL1	−1.18	7.49E-03	intronic antisense
LOC100101148	2.14	3.28E-03	TRIM74	−1.21	4.77E-02	bidirectional
CTD-2168K21.2	−1.57	1.40E-02	NEFL	−1.09	1.17E-02	natural antisense
PF vs CT*						
CTD-2168K21.2	−1.74	3.0E-05	NEFL	−1.53	3.00E-05	natural antisense
RP1–15D23.2	6.22	1.1E-05	TNFSF18	1.14	1.12E-04	intronic antisense
EGFL8	5.45	3.1E-05	NG3	1.97	1.39E-04	exon sense-overlapping
G006280	1.53	2.4E-04	LMOD1	−1.29	1.46E-03	bidirectional
HAND2-AS1	−2.24	3.2E-05	HAND2	−1.72	6.76E-05	bidirectional
G050039	1.14	6.8E-04	NOL4L	−1.26	4.68E-04	Intronic/natural antisense
LOC101929532	1.05	3.5E-04	FAP	−1.78	6.64E-05	natural antisense
G032150	−2.33	4.3E-05	ATP2C2	−1.22	2.15E-04	bidirectional
LOC101926889	−1.69	2.6E-04	ENTPD6	1.42	7.40E-05	intronic antisense
ZFHX4-AS1	−1.15	8.1E-05	ZFHX4	−1.15	4.81E-04	intronic antisense
PF vs P + CT						
G032150	−2.16	1.18E-03	ATP2C2	−1.13	7.06E-03	bidirectional
G061979	−1.09	4.04E-03	SPARCL1	−1.94	7.00E-03	natural antisense
LOC101929572	1.03	3.04E-02	POTEG	1.57	1.49E-02	natural antisense
G035633	1.18	2.50E-02	LOC100134391	1.56	2.03E-02	intronic antisense
RP11-35J23.1	−1.47	2.48E-02	DNTT	1.05	2.14E-02	intronic antisense
LINC00469	−1.20	4.27E-04	LOC100134391	1.56	2.03E-02	intronic antisense
CTD-2313J17.5	1.04	3.72E-02	FAM174B	−1.06	2.59E-03	intron sense-overlapping
RP1-149L1.1	−1.31	8.03E-03	COL9A1	1.26	3.43E-02	natural antisense
G009410	−1.07	1.21E-02	RASSF4	−1.15	2.88E-02	natural antisense

*
The top ten (out of 71) lncRNA/mRNA pairs are shown